

# Statistical thermodynamics of the human brain activity, the Hagedorn temperature and the Zipf law

Dante R. Chialvo<sup>1,2,\*</sup> and Romuald A. Janik<sup>3,†</sup>

<sup>1</sup>*Instituto de Ciencias Físicas (ICIFI-CONICET),  
Center for Complex Systems and Brain Sciences (CEMSC3),  
Escuela de Ciencia y Tecnología, Universidad Nacional de Gral. San Martín,  
Campus Miguelete, 25 de Mayo y Francia, 1650 San Martín, Buenos Aires, Argentina*  
<sup>2</sup>*Consejo Nacional de Investigaciones Científicas y Tecnológicas (CONICET),  
Godoy Cruz 2290, 1425 Buenos Aires, Argentina*  
<sup>3</sup>*Institute of Theoretical Physics and Mark Kac Center for Complex Systems Research,  
Jagiellonian University, ul. Łojasiewicza 11, 30-348 Kraków, Poland*

It is well established that the brain spontaneously traverses through a very large number of states. Nevertheless, despite its relevance to understanding brain function, a formal description of this phenomenon is still lacking. To this end, we introduce a machine learning based method allowing for the determination of the probabilities of all possible states at a given coarse-graining, from which all the thermodynamics can be derived. This is a challenge not unique to the brain, since similar problems are at the heart of the statistical mechanics of complex systems. This paper uncovers a linear scaling of the entropies and energies of the brain states, a behaviour first conjectured by Hagedorn to be typical at the limiting temperature in which ordinary matter disintegrates into quark matter. Equivalently, this establishes the existence of a Zipf law scaling underlying the appearance of a wide range of brain states. Based on our estimation of the density of states for large scale functional magnetic resonance imaging (fMRI) human brain recordings, we observe that the brain operates asymptotically at the Hagedorn temperature. The presented approach is not only relevant to brain function but should be applicable for a wide variety of complex systems.

The proposition that the brain is poised near a critical point of a phase transition suggests that properties universally observed near criticality can be advantageous for brain function. Those include, among the most important, the very large number of metastable states present at criticality, which provides for large memory capacity, also the large susceptibility which may endow the brain with an exquisite sensitivity and at the same time an unlimited dynamic range to process sensory inputs. Finally a rough energy landscape can provide high flexibility for eventual swift changes. Since the hypothesis was put forward by Bak and colleagues [1], considerable experimental support for the main idea has been accumulated, as well as some constructive controversy over technical aspects (see [2–9]). In this paper we focus on a model-independent feature of criticality, specifically in the space of states that the human brain explores during the so called resting conditions (i.e. un-purposeful behaviour) using functional magnetic resonance imaging (fMRI) recordings. According to current understanding, such space of states supposedly represents the brain (microscopic) dynamical repertoire available for perception, cognition and behaviour, hence its physiological importance.

A key characteristic of the system’s space of states is the *density of states* as a function of energy, which determines the thermodynamic behaviour of the system at any temperature, including the existence of criticality. Typically, when studying systems in the thermodynamic limit of infinite size, the system explores only a relatively small portion of the space of states (largest in the critical

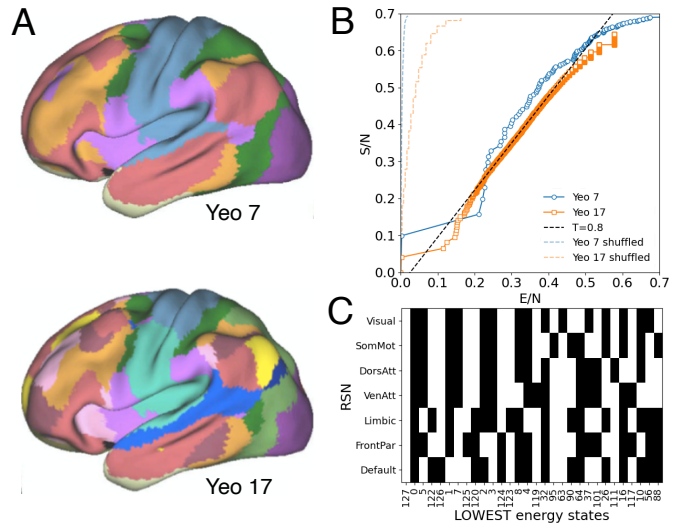


FIG. 1. Entropy-energy dependence (panel B) for very coarse grain fMRI brain data (obtained from the 7 or 17 Yeo’s brain parcellations [20], snapshots shown in panel A) computed by state counting of long concatenated recordings. Dashed lines correspond to results gathered from random shuffled recordings. Panel C shows the 30 lowest (of  $2^7$ ) energy states (with white/black denoting active/inactive) computed for the Yeo’s 7 parcellation.

case). When we deal with a finite but large “mesoscopic” system, however, the repertoire of explored states may be wide enough to encompass information on the behaviour of the system for a range of temperatures. In particu-

lar, it could detect signatures of critical behaviour even away from the system’s operating temperature, hence its determination is of high interest.

The density of states is equivalently expressed in terms of the energy dependence of the (microcanonical) entropy as  $\rho(E) = \exp S(E)$ . A second order phase transition is characterized by  $S''(E_c) = 0$  at some energy  $E_c$  in the thermodynamic limit. Of particular interest for the present paper is the case of a linear dependence  $S(E) \sim aE + b$ . On one hand, as discussed in [2, 10], it is equivalent to Zipf law [11] – a power-law dependence of the probability of a state on its rank. On the other hand, it is known that such exponential increase in the density of states leads to the Hagedorn hypothesis of a limiting temperature [12] (equal here to the inverse slope  $T_H = 1/a$ ), beyond which hadronic matter cannot exist. Since then, Hagedorn temperature appeared in various other contexts in high energy physics [13, 14]. Cabbibo & Parisi [15] found later that similar exponential behaviour can be present in any system which undergoes a second order phase transition, Note that Ref. [2] informally dubbed this behaviour as *very critical*, as then  $S''(E) = 0$  for a whole range of energies.

In this paper, we explore statistical aspects of the space of states of the human brain resting state activity and show the appearance of regimes of linear  $S(E)$  dependence in the entropy-energy plane indicating proximity to a critical point. Moreover, we find that the brain operates asymptotically at the limiting Hagedorn temperature. The present analysis was made possible by a novel machine learning (ML) based method for estimating the density of states from relatively high dimensional data (of the order of hundreds of spins) which we developed as an extension of [3], an approach that should be, in fact, of a very general applicability.

Our considerations are very much model-independent, in particular we do not assume a reduction to pairwise interactions and we admit in principle arbitrary higher order interactions. Our method, however, does not require to specify these interactions explicitly, as they are encoded by the trained machine learning classifiers. The only overall assumption is that we treat the discretized fMRI signals as samples from a Boltzmann distribution at a fixed temperature. This means that the energies of the spin configurations  $\{s_i\}_{i=1}^N$  are given by

$$E(\{s_i\}) = -T \log p(\{s_i\}) + c \quad (1)$$

where  $T = 1$  is typically chosen for convenience and  $c$  is an arbitrary constant, which we set following [10] so that the observed lowest energy state has vanishing energy.

Eq. (1) is very informative as it allows to *extract* the effective Hamiltonian of the system and hence all interactions directly from the probabilities of the particular brain states. Of course, the utility of Eq.(1) depends on the ability of explicitly estimating the state probabilities. As emphasized above, we would like to restrain ourselves

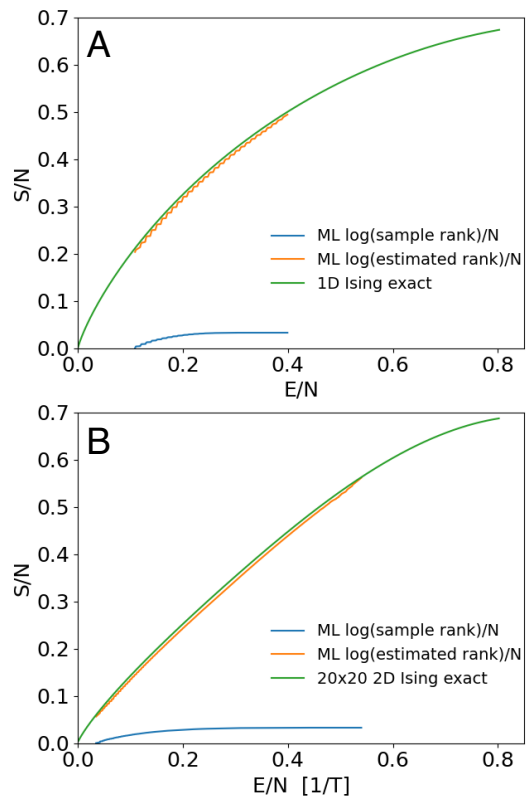


FIG. 2. Verifying the ML method results with the Ising model ground-truth expectations. Entropy-energy plots extracted using the ML method for Monte Carlo simulations of the Ising model. Panel A shows the results for the non-critical 1D Ising ( $T = 1, N = 400$ ) and panel B those for the critical 2D Ising model ( $T = 2.3, N = 400$ ).

from making any *a-priori* assumptions about the form of the Hamiltonian (such as an Ising model with general pairwise couplings, which is the standard starting point for the maximum entropy method [17, 18]).

The remaining ingredient necessary for investigating the existence of linear dependence of entropy on the energy is the (microcanonical) entropy  $S(E)$ . Following the considerations of [2], we identify it with the logarithm of the rank of the corresponding state  $\{s_i\}$  with energy  $E$ :

$$S(E) \simeq \log \text{rank}(\{s_i\}) \quad (2)$$

This relation has the additional benefit that a linear dependence of  $S$  on  $E$  is equivalent to power-like Zipf law linking probability and rank in the space of states [2]. The probability-rank relation is in fact independent of the applicability of the Boltzmann distribution interpretation of the data.

*Brain data.* – We analyzed signals corresponding to fMRI timeseries which measure the level of activation of the brain (as a function of time) simultaneously at several thousands of contiguous locations. We use resting state fMRI data of 100 subjects released by the Hu-

man Connectome Project [1] which once concatenated results in a total of 456000 timesteps (see *Supplementary Information* for detailed information). The brain signals are usually coarse-grained (parcellated) at various scales  $N$  in accordance with functional or anatomical criteria. Fig. 1A illustrates two of the coarser [20] parcellations (also termed regions of interest ROI) of  $N = 7$  and  $N = 17$ , representing so-called Resting State Networks, from which mean time series for each parcel are extracted. Subsequently each signal is transformed into a time series of surrogate spins, by setting the samples above/below the median of each session to +1/-1 (active/inactive) such that the entropy is maximized.

For such heavily coarse-grained cases, the probabilities of all states can be estimated just by counting their number of occurrences. This is the case presented in Fig. 1 which shows that the brain entropy-energy plots, even at this low resolution, already exhibit a region of linear scaling. The slope is above 1, indicating that the corresponding critical (Hagedorn) temperature is *lower* than  $T = 1$ . Note that this is not in contradiction with the concept of the Hagedorn temperature as a limiting temperature, as we are dealing here with a finite system. This result directly shows the appearance of Zipf law/linear scaling for a subset of states without recourse to any nontrivial machine learning based methods. Notice, also, that the low energy vectors (panel C) correspond, as expected, to different degrees of synchronous activation or silence.

To get insight on the system dynamics (in the brain and elsewhere), it is imperative to compute the probabilities from high dimensional sampling. Of course, any naive attempt of doing it from occurrence counts is invalidated by the exponential increase in the number of states, resulting in the vast majority appearing only once in sample data. In order to overcome this difficulty, we adapt a recently developed method of using machine learning classifiers to compute entropy from Monte Carlo samples valid even when all samples are distinct [3]. As the machine learning classifiers used to compute the overall Shannon entropy directly estimate the probability of each state, they are a perfect tool for determining Eq.(1).

*From Machine Learning to state probabilities and ranks.*— We now review briefly the approach of [3] of computing Shannon entropy of high dimensional signals and show how it can be adapted to evaluate the probabilities of individual states, as well as estimating the ranks of states.

The key difficulty in computing the Shannon entropy

$$S_{Shannon} = \langle -\log p \rangle = - \sum_{\alpha} p_{\alpha} \log p_{\alpha} \quad (3)$$

is reliably estimating the  $\log p_{\alpha}$  of states  $\alpha \equiv \{s_i\}_{i=1}^N$  appearing in the data. In the high dimensional case we use machine learning tools to analyze the *internal structure* of the states instead of treating each state as an opaque entity when using occurrence counts. To this end, we

employ the standard decomposition of probability

$$p(s_1, \dots, s_N) = p(s_1)p(s_2|s_1)p(s_3|s_1, s_2) \dots \quad (4)$$

Taking the logarithm, we see that we have to evaluate the conditional probabilities like  $\log p(s_3|s_1, s_2)$ . But this is just what virtually any machine learning classification algorithm provides when predicting the spin  $s_3$  based on  $s_1$  and  $s_2$ . Training  $N$  such classifiers leads to a prescription for  $\log p(s_1, \dots, s_N)$ . Evaluating its average over the data sample gives the estimate of Shannon entropy from [3].

For the purposes of the paper, we need another ingredient which was not present in the considerations of [3], namely evaluating the rank of particular states  $r(\{s_i\})$  appearing in (2). The main difficulty is the fact that the provided data sample contains usually only a very small subset of all possible states, while the rank should be computed in the space of all states.

In order to quantify the unseen states, we will assume that each state from the data sample of a given energy  $E_{\alpha}$  is a representative of some multiplicity of states  $n_{\alpha}^{mult}$  of similar energy in the whole space of states. We estimate these multiplicities by requiring the consistency of computing Shannon entropy from the average of the predicted  $\log p_{\alpha}$  over the provided data sample, as was done in [3], with the one computed purely from the predicted  $p_{\alpha}$ 's and the multiplicities. We thus have

$$- \sum_{\alpha \in data} p_{\alpha}^{empirical} \log p_{\alpha} \simeq - \sum_{\alpha \in data} p_{\alpha} n_{\alpha}^{mult} \log p_{\alpha} \quad (5)$$

where the summation goes over the distinct states present in the data sample and  $p_{\alpha}^{empirical}$  is based on the occurrence count of state  $\alpha$ . The consistency of the two formulas leads to the expression

$$n_{\alpha}^{mult} = \frac{p_{\alpha}^{empirical}}{p_{\alpha}} \quad (6)$$

The estimate of the true rank is then obtained as the cumulative sum of the multiplicities leading to

$$S(E) \simeq \log \sum_{E_{\alpha} \leq E} n_{\alpha}^{mult} \quad (7)$$

*Testing the ML method with the Ising model.*— In order to test the proposed ML method for obtaining the density of states, we applied it to the exactly solvable 1D and 2D Ising models with  $N=400$  spins, which have similar dimensionality as the parcellated brain data and are respectively either always noncritical or close to criticality (evaluated here at  $T = 2.3$ ). The results are shown in Fig. 2 (see more checks in the Supplementary Information [? ]). Here, the arbitrary constant  $c$  in (1) was adjusted to agree with the conventions of the Ising models used for the ground-truth  $S(E)$  curves. For the  $N = 400$  dimensionality, the vast majority of states are

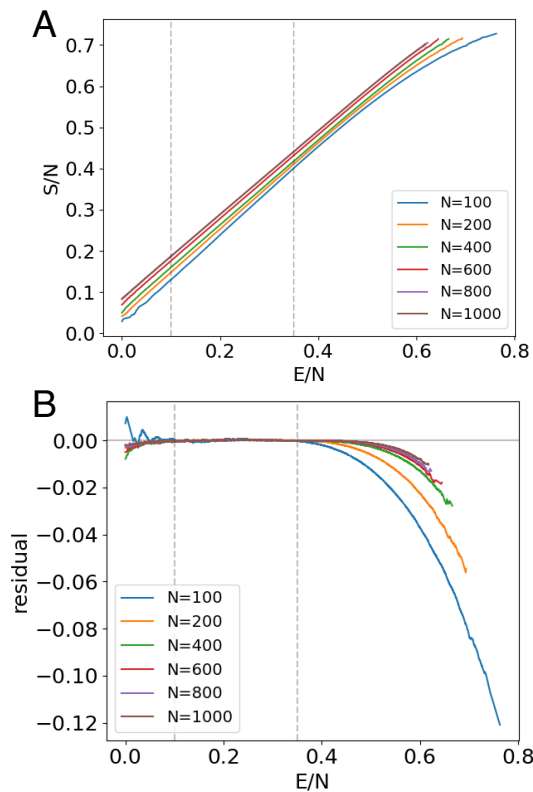


FIG. 3. Panel A: Entropy-energy plots for resting state fMRI data with Schaefer parcellations of varying sizes. Panel B: The residuals of the linear fits performed between the two dashed lines.

unobserved, so the estimate of the multiplicity (6) is crucial for obtaining the correct result in Fig. 2. Indeed, ignoring the multiplicities and using just the naive ranks of the observed states in the data, not only severely underestimates the entropy, but also leads to a different functional shape of the energy dependence (see the blue versus orange curves in Fig. 2).

*Brain fMRI resting state data results.* – As commented above, for parcellations with small  $N$ , we can estimate the state probabilities just from the occurrence counts and directly compute the corresponding ranks. In fact, the case of  $N = 17$  shown in Fig. 1 is at the borderline of the applicability of the direct methods, as we found that only  $\sim 43\%$  of the possible states occur in the data.

Now we proceed to the main challenge of the paper, which is to identify the states for much finer parcellations. First, we consider the family of Schaefer parcellations constructed in [21], as they come in variants ranging from  $N = 100$  to  $N = 1000$  ROIs. Such parcellated time-series contain only a very small fraction of all the possible states and even for the smallest  $N = 100$  case, we found that  $\sim 98\%$  of the states in the data appear only once. Thus we have to employ the machine learning method described earlier in the paper. We use a state-of-the-art

nonlinear classifier `xgboost` [2] with settings as in [3] (see Supp. Info. [?] for details).

The exploration of the Schaefer parcellations for a variety of  $N$ s (see Fig. 3A) reveals a linear behaviour whose range increases with  $N$  (see Fig. 3B), confirming the observation made for the  $N = 17$  Resting State Networks shown in Fig.1B.

As a further test of the robustness of the results, we constructed a set of parcellations applying the Phenomenological Renormalization Group (PRG) approach of [23] resulting in subdivisions with  $N = 62, 124, 249$  and 499 ROIs, out of 998 ROIs of the  $N = 1000$  Schaefer parcellation. PRG parcellations differ from the Schaefer ones in that they are constructed following correlation hierarchies and often group together ROIs lying in different brain hemispheres. Remarkably, the critical temperatures extracted from the PRG subdivisions are very much in line with the expected values from the Schaefer parcellations (see Fig. 4B). The qualitative observation of the critical (Hagedorn) temperature approaching  $T = 1$  with increasing  $N$  is quantitatively confirmed by the power law

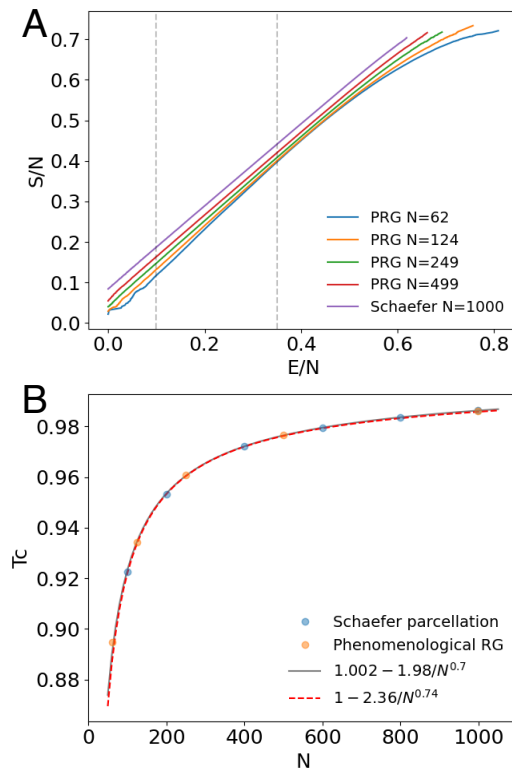


FIG. 4. Panel A: Entropy-energy plots for brain data successively coarse-grained using Phenomenological RG. Panel B shows the Hagedorn temperature extracted from the inverse slope of the linear fits as a function of parcellation granularity for both the PRG and the Schaefer parcellations (i.e., the data in Fig. 3A). In both cases temperature scales with  $N$  as a power law (the power law fits denoted in the legends were performed only using the Schaefer parcellations).

fits shown in Fig. 4B. This indicates that, asymptotically at a fine-grained level, the brain effectively operates at the Hagedorn temperature with a very large repertoire of brain states satisfying Zipf law. This is one of the key results of the present paper.

A finding consistent with the appearance of the linear  $S(E)$  regime close to  $T = 1$ , is the observation that the range of energies (scaled by  $N$ ) present in the data sample is remarkably stable with increasing  $N$ . This is in marked contrast with the conventional picture in statistical physics where the range markedly decreases with  $N$ , especially away from a critical point. Indeed, a linear dependence of  $S(E) \sim E/T_H + b$  between  $E_0$  and  $E_1$  means that at  $T = T_H$ , all energies between  $E_0$  and  $E_1$  are equally likely to occur. This follows from rewriting the partition function as

$$Z(T) = \int dE e^{S(E) - E/T} \quad (8)$$

Going back to the probabilistic interpretation of Eq. (1), this means that even for a large system, states with a wide range of probabilities nevertheless still occur, endowing the system with a very *diverse* dynamical repertoire, a fundamental property which in neurobiology is interpreted as the required microscopic basis of a rich (macroscopic) cognitive behaviour.

A number of checks (see Supp. Info. [? ]) further confirmed the robustness of the results, including decorrelating the data, testing the stability w.r.t. the filtering of the fMRI data, and the degree of scale-invariance of successive parcellations.

Summarizing, the analysis of large scale fMRI brain recordings via a machine learning approach shows the existence of a robust region of a linear  $S(E)$  regime, whose range and proximity to the “operating temperature”  $T = 1$  increases with the dimensionality of the sampling  $N$ , i.e. going to finer and finer length-scales. This leads to the finding that the brain operates asymptotically at the Hagedorn temperature. The appearance of the linear  $S(E)$  dependence demonstrates that a wide range of brain states follow Zipf’s law. The approach presented in this paper on one side allowed the first empirical demonstration of the wide linear regime of a very diverse (critical) density of brain states – fundamental for normal brain function – and on the other offers a powerful tool to study other complex systems.

*Acknowledgments.*– This work was conducted under the auspices of the Jagiellonian University-UNSAM Cooperation Agreement and supported by Grant No. 1U19NS107464-01 from the NIH BRAIN Initiative, by CONICET (Argentina) and Escuela de Ciencia y Tecnología, UNSAM, (Argentina) and by the Foundation for Polish Science (FNP) project TEAMNET “Bio-inspired Artificial Neural Networks” (POIR.04.04.00-14DE/18-00). RJ was also supported by a Priority Re-

search Area DigiWorld grant under the Strategic Programme Excellence Initiative at the Jagiellonian University (Kraków, Poland).

\* dchialvo@gmail.com

† romuald.janik@gmail.com

- [1] P. Bak, *How Nature Works: The Science of Self-Organised Criticality*. (Copernicus Press, New York, 1996).
- [2] T. Mora & W. Bialek, *J. Stat. Phys.* **144**, 268–302 (2011).
- [3] D.R. Chialvo, *Nat. Phys.* **6**, 744 (2010).
- [4] M.A. Muñoz. *Rev. Mod. Phys.* **90**, 031001 (2018).
- [5] J.M. Beggs & N. Timme, *Front. Physiol.* **3**, 163 (2012).
- [6] J.M. Beggs & D. Plenz. *J.Neurosci.* **23**,11167–11177 (2003).
- [7] A. Haimovici, E. Tagliazucchi, P. Balenzuela, and D.R. Chialvo, *Phys. Rev. Lett.* **110**, 178101 (2013).
- [8] E. Tagliazucchi, P. Balenzuela, D. Fraiman and D.R. Chialvo, *Front. Physiol.* **3**, 15 (2012).
- [9] S. Camargo, D.A. Martin, E.J. Aguilar Trejo, A. de Florian, M.A. Nowak, S.A. Cannas, T.S. Grigera and D.R. Chialvo, *Phys. Rev. E* **108**, 034302, (2023).
- [10] G.J. Stephens, T. Mora, G. Tkacik, W. Bialek, *Phys. Rev. Lett.* **110**, 018701 (2013).
- [11] G.K. Zipf, *The Psycho-biology of Language*. (Houghton-Mifflin, Boston, 1935).
- [12] R. Hagedorn, *Nuovo Cim. Suppl.* **3**, 147 (1965).
- [13] J.J. Atick, E. Witten, *Nucl.Phys. B* **310** 291–334 (1988).
- [14] O. Aharony, J. Marsano, S. Minwalla, K. Papadodimas, M. Van Raamsdonk, *Adv.Theor.Math.Phys.* **8**, 603–696 (2004) [arXiv:hep-th/0310285].
- [15] N. Cabibbo & G. Parisi. *Phys.Lett. B* **59**, 67–69 (1975).
- [16] R.A. Janik, arXiv:1909.10831
- [17] E. Schneidman, M. Berry, R. Segev, W. Bialek *Nature* **440**, 1007–1012 (2006).
- [18] Y. Roudi, S. Nirenberg, P.E. Latham *PLOS Computational Biology* **5**, 5, e1000380 (2009).
- [19] D.C. Van Essen, S.M. Smith, D.M. Barch, T.E.J. Behrens, E. Yacoub, K. Ugurbil, *NeuroImage* **80**, 62–79 (2013).
- [20] B.T.T. Yeo, F.M. Krienen, J. Sepulcre, M.R. Sabuncu, D. Lashkari, M. Hollinshead, J.L. Roffman, J.W. Smoller, L. Zöllei, J.R. Polimeni, B. Fischl, H. Liu, and R.L. Buckner. *J. Neurophysiol.* **106**, 1125–1165 (2011).
- [21] A. Schaefer, R. Kong, E.M. Gordon, T.O. Laumann, X.N. Zuo, A.J. Holmes, S.B. Eickhoff and B.T.T. Yeo, *Cerebral Cortex* **28**, 3095–3114 (2018).
- [22] <https://github.com/dmlc/xgboost>
- [23] L. Meshulam, J.L. Gauthier, C.D. Brody, D.W. Tank, and W. Bialek, *Phys. Rev. Lett.* **123**, 178103 (2019).

## Supplementary information

We include here additional information concerning technical details of the fMRI data pre-processing, checks for the robustness of the results and additional observations.

**fMRI data.** We used the ICA-FIX cleaned resting-state fMRI data for 100 unrelated subjects from the Human Connectome Project [1] Young Adult dataset downloaded from <https://www.humanconnectome.org/study/hcp-young-adult>. This includes 4 sessions of approximately 15 min duration each, collected with  $TR=0.72s$ . The resulting data were subsequently detrended, band-pass filtered in the range 0.01-0.25Hz and normalized to zero mean and unit standard deviations (using `nilearn.signal.clean`). The first and last 30 frames were dropped, resulting in 1140 frames for each of the 400 sessions. In this way we obtain timeseries of 456000 datapoints length. Binarization was performed for each session individually, i.e. always using the medians of the specific session as thresholds.

**Further Ising model tests.** In order to test our method of estimating entropy and energy from a provided set of spin configurations, we performed Monte Carlo simulations using the Metropolis algorithm of the 1D Ising model with  $N = 100$  and  $N = 400$  spins at  $T = 1$  and the 2D Ising model on  $10 \times 10$  and  $20 \times 20$  lattices. In order to have comparable overall statistics to the HCP brain fMRI data, in each case we generated 400 sessions of 1140 samples, starting each session from a different random initialization. We used 1000 and 4000 thermalization steps between the MC samples for the models with 100 and 400 spins respectively. In Fig. S1, we show results for the 1D and 2D models with  $N = 100$  spins. In addition, we directly compare the energies of all individual states present in the MC data to the values predicted by our machine learning algorithm using the `xgboost` classifier.

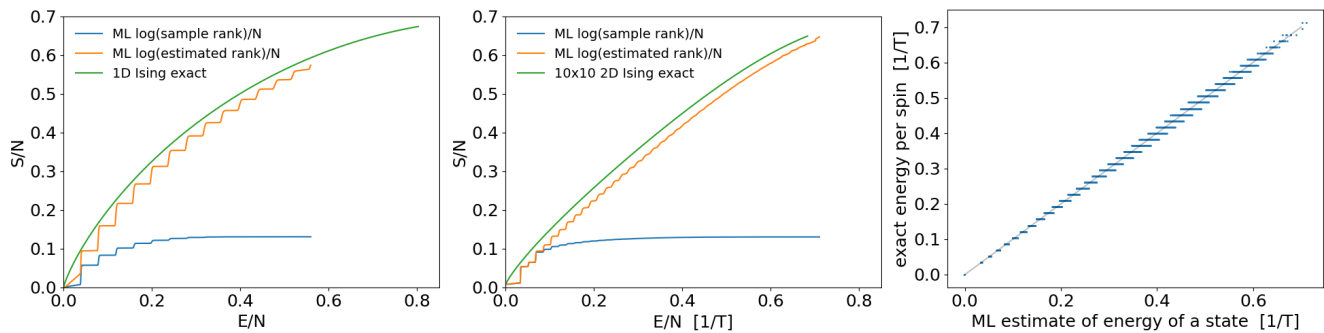


FIG. S1. Further tests of the machine learning method for systems with  $N = 100$  spins: noncritical 1D Ising model at  $T = 1$  (left), critical 2D Ising model at  $T = 2.3$  (center), comparison of the energies of states extracted from the Monte Carlo data of the 2D Ising model by the machine learning algorithm with the true energies (right).

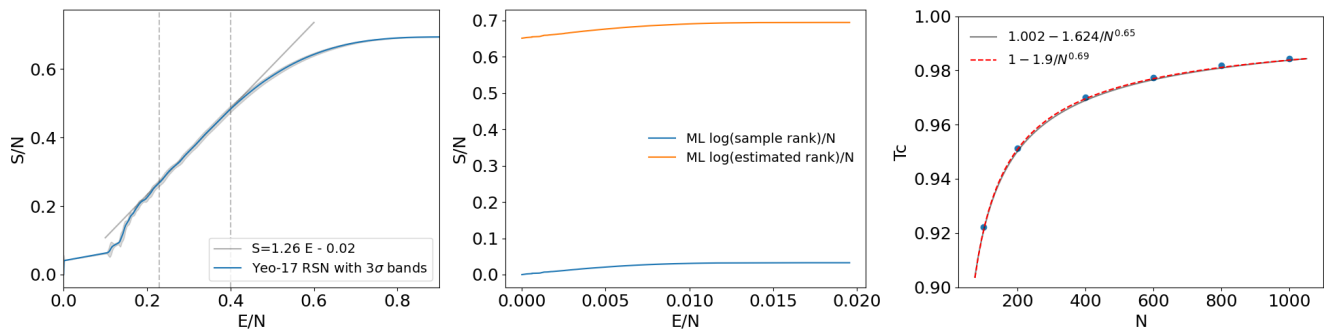


FIG. S2.  $3\sigma$  error bands for the entropy-energy plot for Yeo-17 RSN from 1000 bootstrap datasets (left).  $N = 400$  parcellation data with each ROI's signal randomly shifted, thus decorrelating the data. Note the very narrow range of energies (probabilities) on the horizontal axis. The predicted probabilities for all states are in the vicinity of  $1/2^{400}$  (center). Extraction of the critical (Hagedorn) temperature as a function of  $N$  from fMRI data with no low-pass filtering. (right).

**Bootstrap, randomization and robustness tests.** For the Yeo-17 RSN, we performed a bootstrap estimation of the statistical errors. Bootstrap was performed on the session level, i.e. we generated 1000 bootstrap datasets by repeatedly randomly selecting 400 sessions with replacement. The entropy-energy curve was obtained by training the `xgboost` classifiers on each whole bootstrap dataset and subsequently predicting the energies of all  $2^{17}$  states in the state-space. The results are shown in Fig. S2(left). The entropy-energy curve appears remarkably robust. The determination of the slope is  $1.2559 \pm 0.0082$ , which translates to the critical temperature  $0.7963 \pm 0.0052$ .

In order to compare the obtained results with the case of a lack of internal structure of the states, we decorrelated the signals of all ROIs (performed here for the  $N = 400$  Schaefer parcellation) by concatenating the sessions, randomly cyclically shifting the signal of each ROI and then again splitting into sessions. The resulting entropy-energy curve is shown in Fig. S2(center). The range of energies (probabilities) is very narrow and is concentrated around  $1/2^{400}$  (this value is not seen on the plot as we use the convention of setting the energy of the lowest observed state to zero). Such a behaviour is clearly very different from any brain data we studied.

In order to test the influence of filtering of the fMRI data on our results, we repeated the computations leading to asymptotic scaling of the critical temperature with the number of ROIs without performing any low-pass filtering. The result is shown in Fig. S2(right), which is an analog of Fig.4B in the main text. We observe that the conclusion of the brain operating asymptotically at the Hagedorn temperature still holds with a high accuracy. The scaling exponent is 0.69 (in comparison with 0.74 there) – both are consistent with a rough value of 0.7. Indeed, comparing the two fits for each set of data, we see that the scaling exponent is reliable to the leading decimal digit.

**Phenomenological Renormalization Group (PRG).** The PRG construction operates on the initial *non-binarized* data. In the present paper, we start with the fMRI data parcellated in the  $N=1000$  Schaefer parcellation, which for the HCP data has actually 998 nonempty ROIs. We compute the  $998 \times 998$  correlation matrix, identify the pair  $i, j$  of ROIs with maximal correlation and form a new signal

$$y_1(t) = \frac{1}{2} (x_i(t) + x_j(t)) \quad (9)$$

We then repeat the process with the remaining ROIs, constructing further  $y_k(t)$  until we exhaust all ROIs or a single one remains. In the latter case we drop it. Repeating the above procedure iteratively, we obtain PRG datasets of dimensionality  $N=499, 249, 124$  and  $62$ . For further analysis, we binarize them exactly as the original parcellated data.

**Data scale-invariance.** Let us comment on the relation of the extracted state energies associated with the fMRI data coarse-grained with different granularity. In Fig. S3, we compare the predicted energies for the individual fMRI timesteps between Schaefer parcellations of sizes differing by a factor of two. We observe a consistency of the predicted energies (defined here as  $-\log p$  without any subtraction) normalized to the size of the system. In Fig. S4, we observe a similar behaviour when applying the Phenomenological Renormalization Group construction to the  $N = 1000$  Schaefer parcellation. These results can be interpreted as a signature of approximate scale invariance of the system, as we can think of this computation as a comparison of hamiltonians in various coarse-grainings in the Renormalization Group sense.

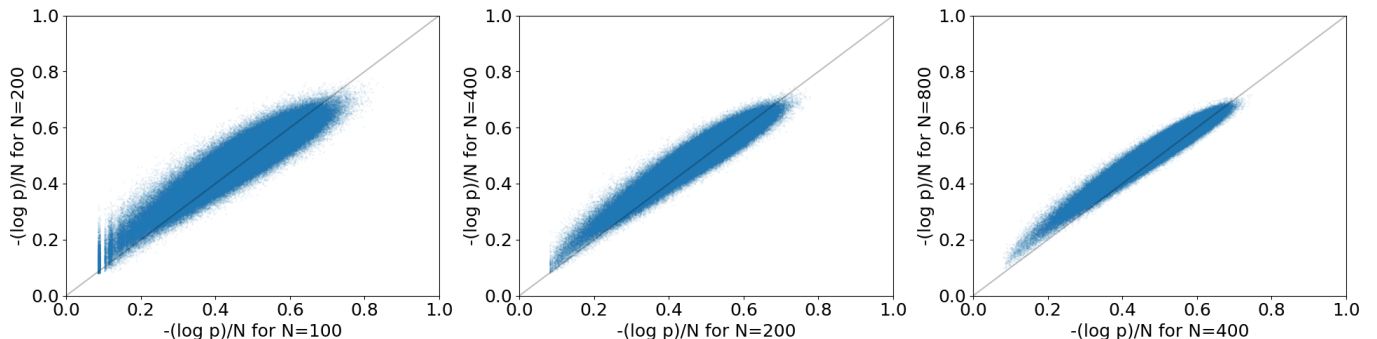


FIG. S3. Comparison of the predicted probabilities (energies) for the same states using Schaefer parcellations with  $N$  differing by factors of two. The slight systematic deviation of the point clouds from a unit slope suggests that the effective operating temperatures at the corresponding  $N$ s are slightly different.

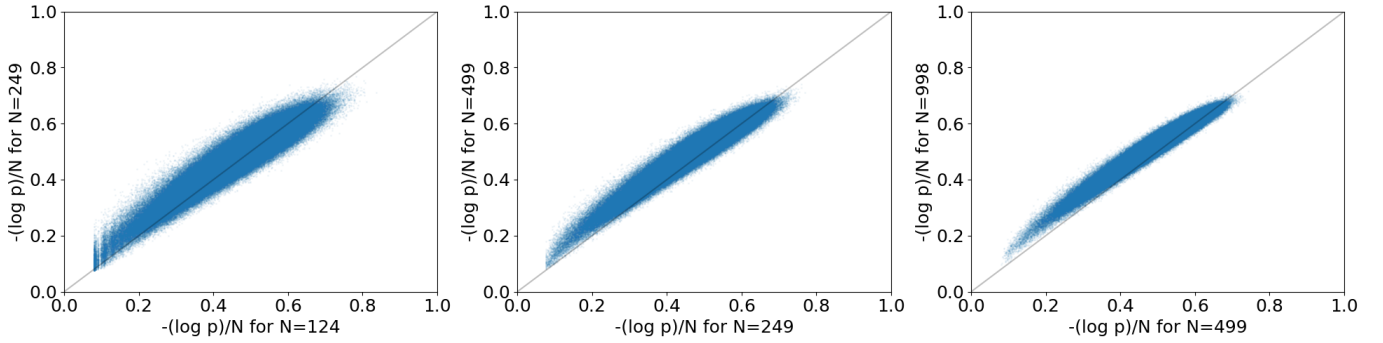


FIG. S4. Comparison of the predicted probabilities (energies) for the same states using consecutive steps of the Phenomenological Renormalization Group (PRG).

**Details on the machine learning method.** In all applications of the machine learning method we use the `xgboost` classifier [2], with the settings from [3], which were optimized for a  $20 \times 20$  2D Ising model, i.e. `max_depth=3` and `n_estimators=50`. The computations were done on a GPU employing `tree_method='hist'` for efficiency. As the code [4] released with ref. [3] was dedicated just for computing the overall entropy of the data, we provide below the pseudo-code for computing the logarithms of probabilities of the individual samples from the data. In principle one can use here any machine learning classifier which returns probabilities of the predicted class. The quality of the classifier or its parameters can be assessed by evaluating the Shannon entropy from the obtained probabilities and choosing the classifier or its settings which yield the lowest entropy.

---

**Algorithm 1** Estimate the probabilities of individual samples in the provided data

---

- 1: **Input:** binary data  $X^{all}$  of size  $S \times T \times N$ ,  
number of sessions  $S$ ,  
number of timesteps in a session  $T$ ,  
dimensionality  $N$
  - 2: **Output:** logarithms of probabilities of all states:  $logp$  of size  $S \times T$
  - 3: extract the first spin  $y_{s,t} \equiv X_{s,t,1}^{all}$
  - 4: compute probability of the first spin  $p_1 = mean(y)$
  - 5: initialize  $logp_{s,t} = y_{s,t} \log p_1 + (1 - y_{s,t}) \log(1 - p_1)$
  - 6: **for**  $i = 2$  **to**  $N$  **do**
  - 7:   construct training data for predicting spin  $i$ :  $X = X_{:::,1..i-1}^{all}$
  - 8:   construct target for predicting spin  $i$ :  $y = X_{:::,i}^{all}$
  - 9:   randomly split the sessions into 5 training and testing cross-validation (CV) folds
  - 10:   **for**  $X^{train}, y^{train}, X^{test}, y^{test}$  in each CV fold **do**
  - 11:     train a ML classifier  $clf$  to predict  $y^{train}$  from  $X^{train}$
  - 12:     predict probabilities for the samples in  $test$ :  $p^{test} = clf(X^{test})$
  - 13:     update  $logp$  in the  $test$  subset of the data:  

$$logp^{test} \rightarrow logp^{test} + y^{test} \log p^{test} + (1 - y^{test}) \log(1 - p^{test})$$
  - 14:   **end for**
  - 15: **end for**
- 

For performing the analysis of the present paper, we need the probabilities of *distinct* states  $\alpha$  in the data, thus extracting the subset of the results  $p_\alpha$  returned by the algorithm corresponding to these distinct states. Moreover, in order to estimate the multiplicities in Eq. (6) in the main text, we need also the occurrence counts of these distinct states to get

$$p_\alpha^{empirical} = \frac{\text{occurrence count of state } \alpha \text{ in data}}{\text{total number of samples}} \quad (10)$$

Consequently, we may estimate the Shannon entropy of the data through

$$S \equiv -\langle \log p \rangle = - \sum_{\text{distinct } \alpha} p_\alpha^{empirical} \log p_\alpha = -\frac{1}{ST} \sum_{s,t} \log p_{s,t} \quad (11)$$



The github repository [https://github.com/rmldj/brain\\_hagedorn\\_paper](https://github.com/rmldj/brain_hagedorn_paper) contains the code and the binarized fMRI data to reproduce the examples in Figure 1 of the paper.

---

\* [dchialvo@gmail.com](mailto:dchialvo@gmail.com)

† [romuald.janik@gmail.com](mailto:romuald.janik@gmail.com)

- [1] Data were provided by the Human Connectome Project, WU-Minn Consortium (Principal Investigators: David Van Essen and Kamil Ugurbil; 1U54MH091657) funded by the 16 NIH Institutes and Centers that support the NIH Blueprint for Neuroscience Research; and by the McDonnell Center for Systems Neuroscience at Washington University.
- [2] <https://github.com/dmlc/xgboost>
- [3] R.A. Janik, Entropy from Machine Learning, arXiv:1909.10831
- [4] <https://github.com/rmldj/ml-entropy>